Experimental Investigation of Deconstructable Steel-Concrete Shear Connections in Sustainable Composite Beams

Lizhong Wang[1], Mark D. Webster[2], and Jerome F. Hajjar[3]

[1] Graduate Research Assistant, Department of Civil and Environmental Engineering, Northeastern University, Boston, MA 02115; PH (617)775-9809; Email: wang.l@husky.neu.edu
[2] Senior Staff II – Structures, Simpson Gumpertz & Heger Inc., Waltham, MA 02453; PH (781)907-9369 ; Email: MDWebster@sgh.com
[3] CDM Smith Professor and Chair, Department of Civil and Environmental Engineering, Northeastern University, Boston, MA 02115; PH (617)794-7844; Email: JF.Hajjar@neu.edu

ABSTRACT

A new deconstructable composite floor system consisting of precast concrete planks and deconstructable clamping connections is proposed to promote sustainable design of composite flooring systems in steel buildings through reuse of the structural components. This paper presents an experimental testing program to demonstrate the strength and ductility of the deconstructable connectors and the behavior of the structural floor framing system.

INTRODUCTION

Steel-concrete composite floor framing systems remain one of the most cost-effective forms of construction. The benefits of composite beams and floors include enhanced flexural strength and stiffness, reduced steel beam size and weight, and ease of construction. However, in the traditional composite floor systems, the steel beams and concrete slabs cannot be readily separated because the concrete is cast integrally with the shear studs welded to the beam flange. Hence, steel beams are commonly recycled, and concrete slabs are sent to landfill or downcycled to aggregate. As the need to reduce the energy consumption and material waste related to the building industry increases, it is crucial to reclaim materials from renovation and demolition projects and reuse the salvaged materials in new buildings.

A deconstructable composite floor system is proposed which enables sustainable design of composite beams and floors, deconstruction of buildings, and reuse of the structural components. Figure 1 illustrates the deconstructable composite beam prototype; this concept was first introduced in Webster et al. (2007). The system consists of precast concrete planks and steel beams connected using clamping connectors. Composite action is achieved by utilizing the frictional forces generated at the steel-concrete interface to resist the required shear flow. By loosening the bolts, the precast concrete planks and the steel beams can be easily disassembled and reconfigured in future projects. To ensure structural integrity under lateral loading, unbonded threaded rods are employed to connect the precast concrete planks. Grouting planks and placing a cast-in place concrete topping, which are common in

current precast construction and inhibit the separation and deconstruction of the planks, are avoided. Figure 2 illustrates a pattern of connections spaced every 4 ft. The plank end joints are staggered for construction flexibility and to facilitate in-plane diaphragm force transfer.

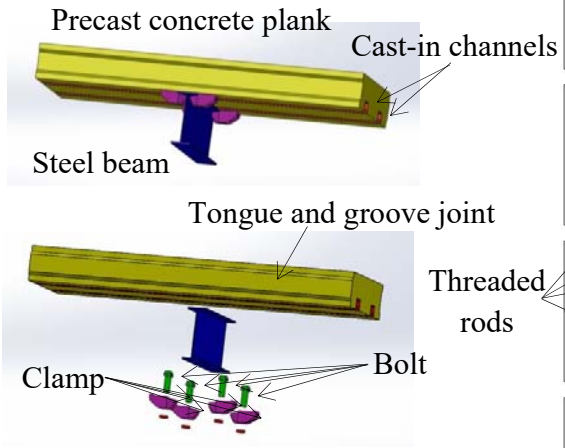

Figure 1. Deconstructable Composite Beam Prototype

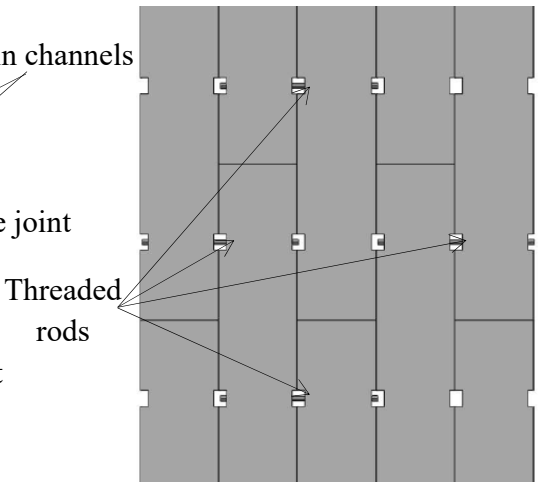

Figure 2. Precast Concrete Plank Connections

In this paper, an experimental testing program is presented which investigates the strength and ductility of the deconstructable shear connectors. Full-scale composite beam tests are also designed and will be conducted to demonstrate the flexural behavior of the system.

EXPERIMENTAL PROGRAM

Pushout Tests

The pushout test program includes two series of tests. In the pretension tests, the number of turns of the nut was first determined to ensure adequate and reliable axial forces generated in the bolts. Pushout tests were then performed to study the strength and ductility of the clamping connectors and explore the influences of the testing parameters.

Pretension test

The clamping system uses T-bolts inserted into cast-in channels. Because the cast-in channels can deform significantly when the bolts are pretensioned, more turns of the nut than in standard bolted connections are needed to enable the bolts to deform into the inelastic range and meet minimum pretension requirements in the AISC specification (2010a). Three M24 and M20 bolts were tested under torqued tension until fracture to develop the relationship between the number of turns and the bolt axial force. The pretension test setup is shown in Figure 3. During the test, while the nut was turned for the tested bolt, the other three bolts were in a snug-tight condition.

After locally removing the threads, strain gages were attached to the shanks of the tested bolts to monitor the axial strain variations. All the bolts fractured after 5 complete turns. The failure modes are shown in Figure 4. The plots in Figure 5 show that the bolt tension increase becomes less for the same amount of nut rotation, indicating that the bolts are inelastic. Two turns and 1.5 turns after a snug-tight condition were selected for pretensioning the M24 and M20 bolts, respectively.

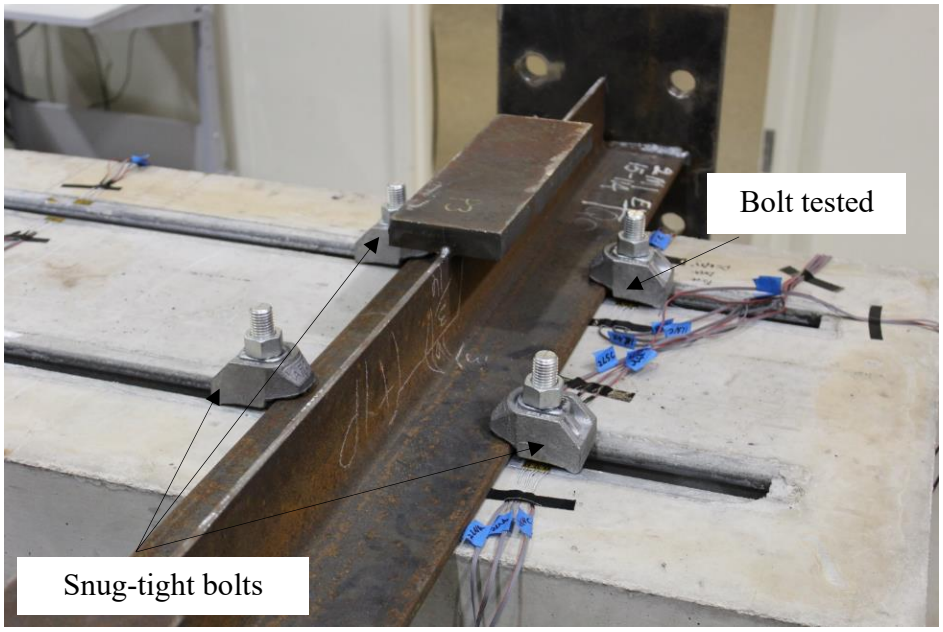

Figure 3. Pretension Test Setup

From right to left: Bolt1, Bolt2, and Bolt 3

a) M24

From right to left: Bolt1, Bolt2, and Bolt 3

b) M20

Figure 4. Fracture of Bolts in Pretension Test

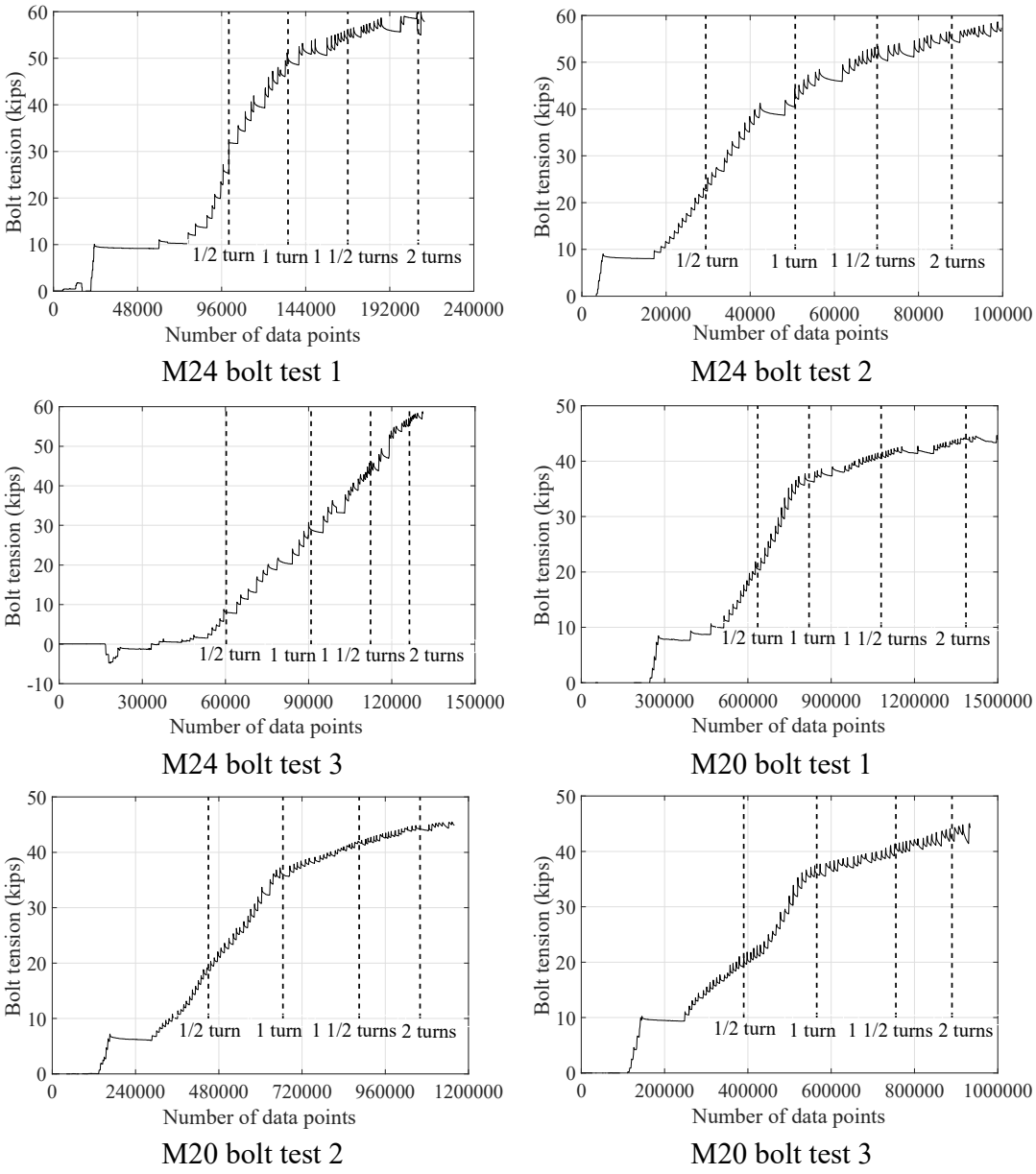

Figure 5. Bolt Tension Variation

Pushout Test

- Test Setup

A self-reacting frame was utilized for the pushout tests. The specimens consisted of 4 ft. × 2 ft. × 6 in. precast concrete planks attached to WT5x30 or WT4x15.5 sections using clamping connectors. WT5x30 and WT4x15.5 sections represent typical floor beams with different flange thicknesses, with the larger WT tested with M24 clamps and the smaller WT tested with M20 clamps. The WT4x15.5 sections were also used with M24 clamps, requiring shims between the clamps and

the WT flange since the flange was relatively thin. The concrete planks were mounted upside down for viewing the motions of the beams and clamps during the tests. Detailed dimensions of the test setup are given in Figure 6. Parameters for the pushout tests include bolt diameter, number of channels, reinforcement configuration, loading protocol, and usage of shims (Table 1). Because the concrete plank used for the pretension tests was regarded as the first specimen, the numbering of the specimens in Table 1 started from 2. The specimen naming convention is explained using Test 6-m24-2c-h-c-s, with m24 describing M24 bolts, 2c describing two channels embedded in the concrete plank, h describing heavy reinforcement configuration, c describing cyclic loading, and s describing shims. In the lightly reinforced specimens, the reinforcement was designed only for gravity loading. Additional supplementary reinforcement was placed around the channel anchors to prevent anchor-related failures in the heavily reinforced specimens. The number of turns of the nut applied to the bolts in the specimens after a snug-tight position is shown in the last column of the table. More details about the test setup and different reinforcement patterns can be found in Wang et al. (2015).

Table 1. Pushout Test Matrix

Test	Test parameters										Number of turns
	Bolt diameter		Number of channels		Reinforcement configuration		Loading		Shim		
	M24	M20	2	3	Light	Heavy	Monotonic	Cyclic	Yes	No	
2-m24-2c-h-m	✓		✓			✓	✓			✓	3 turns
3-m24-2c-l-c	✓		✓		✓			✓		✓	2 turns
4-m24-2c-h-m-s	✓		✓			✓	✓		✓		3 turns
5-m24-2c-h-c	✓		✓			✓		✓		✓	2 turns
6-m24-2c-h-c-s	✓		✓			✓		✓	✓		2 turns
7-m24-3c-h-m	✓			✓		✓	✓			✓	2 turns
8-m24-3c-h-c	✓			✓		✓		✓		✓	2 turns
9-m20-2c-h-m		✓	✓			✓	✓			✓	1.5 turns
10-m20-2c-h-c		✓	✓			✓		✓		✓	1.5 turns

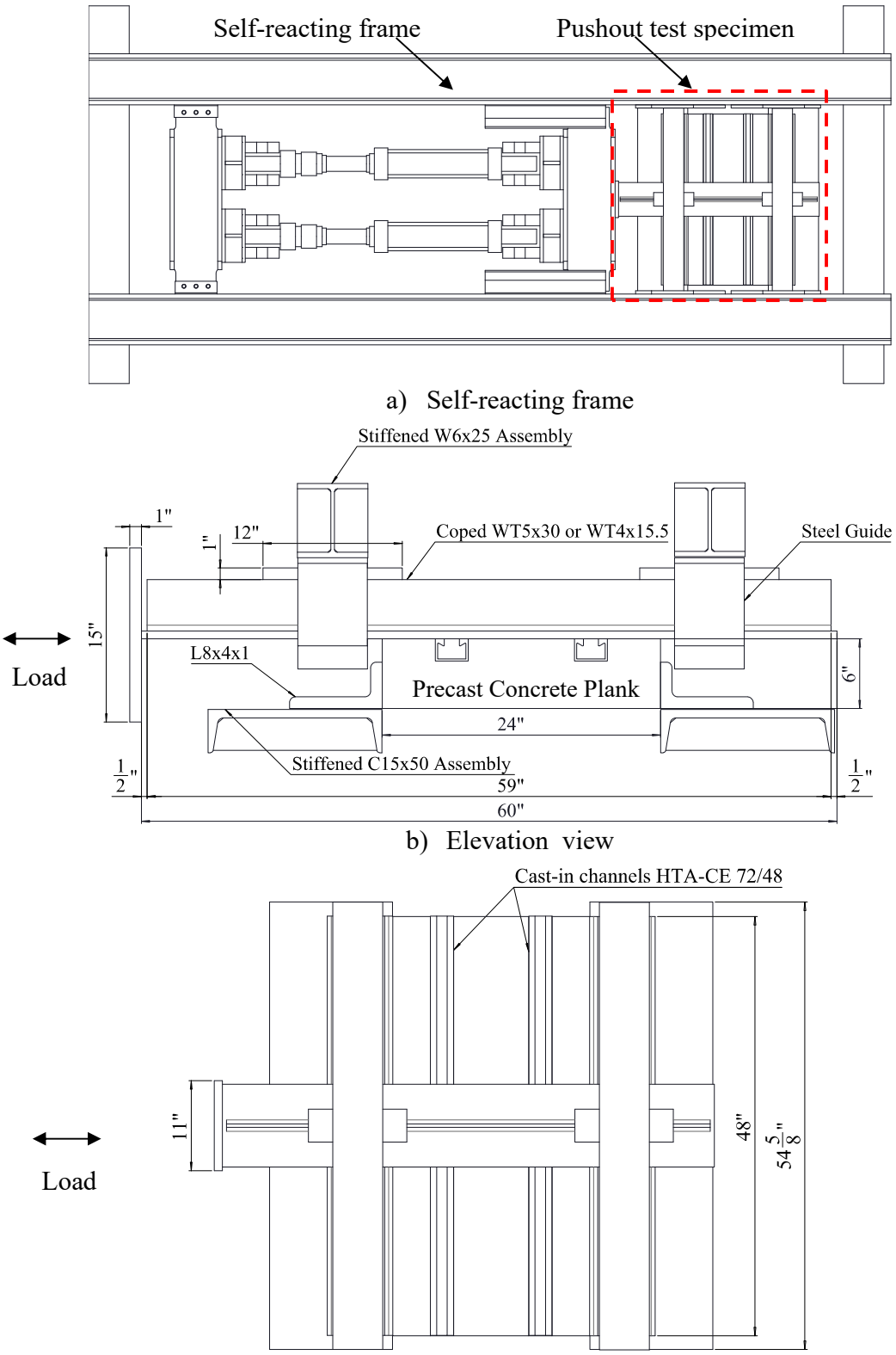

Figure 6. Different Views of Pushout Test Specimen

- Material Tests

In the pretension tests and pushout tests, all materials of the same size were from the same heat. Round coupons were machined from the bolts. Tensile testing was also conducted on dogbone-shaped coupons cut from the flange and web of the embedded channels. The tested material properties of the steel components are given in Table 2. The average compressive strength and splitting tensile strength of the cylindrical concrete specimens are shown in Table 3.

Table 2. Material Properties of the Steel Components

Specimen		Elastic Modulus (ksi)	Yield Strength (ksi)	Ultimate Strength (ksi)
Channel	Flange	28000	67.2	72.2
	Web	27800	62.0	66.6
Bolt	M24	31000	119.7	136.4
	M20	30900	116.9	132.8

Table 3. Compressive and Splitting Tensile Strength of Concrete

Specimen #	Compressive (psi)		Splitting tensile(psi)
	28 days	Test day	28 days
1-3	4,203	6,365	383
4-6		6,446	
7-10		5,883	

- Loading Protocol

The monotonic tests were displacement-controlled. Since the load-slip curves showed gradual changes in response, the load corresponding to a slip of 0.02 in. was defined as the slip load, in accordance with the RCSC Specification (RCSC 2009). The cyclic loading history is depicted in Figure 7. The AISC loading protocol for beam-to-column moment connections was used as a guide for establishing a cyclic loading history for the clamped connections. The first three levels were controlled by forces, using 37.5%, 50% and 75% of the slip load, which was obtained from the corresponding monotonic test, specified as levels 1, 2, and 3, respectively. Slip was then used to control the rest of the test. The loading rates shown in Figure 7 were adopted in both monotonic and cyclic tests, except that the loading rate was 0.0025 in. per minute until a slip of 0.02 in. was attained in the monotonic tests.

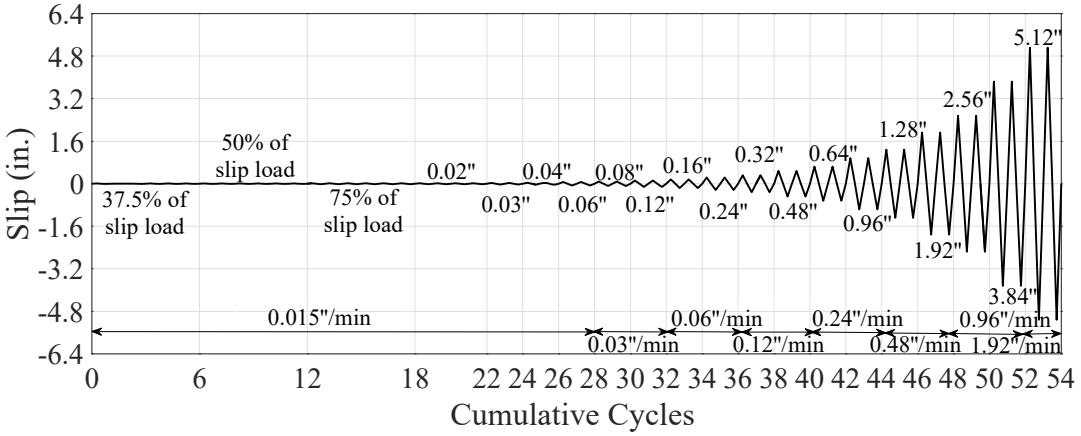

Figure 7. Pushout Test Cyclic Loading History

- Test Results

The load-slip curves of all the monotonic and cyclic specimens are plotted in Figure 8. Three complete turns of the nut were used for the bolts in Tests 2-m24-2c-h-m and 4-m24-2c-h-m-s, which were performed first; however, this rotation was excessive and led to bolt head fracture in Test 4-m24-2c-h-m-s, which is indicated by the sharp strength drop at a slip of just under 1 in. The tests were all terminated when the maximum slip that could be measured by the linear potentiometers was reached. No specific limit states were observed for all the monotonic specimens.

The monotonic test results are summarized in Table 4. For each test, the slip load and peak load are both normalized relative to Test 2-m24-2c-h-m. The slip strength and peak strength of Test 7-m24-3c-h-m in which three channels were used were approximately 50% higher than those of Test 2-m24-2c-h-m, which used two channels, implying that the shear force could be distributed among the clamps. In Test 9-m20-2c-h-m, M20 bolts were tested, and the strength was about 60% of Test 2-m24-2c-h-m using M24 bolts. Nevertheless, the M20 bolts could not maintain their strength as well as the M24 bolts, as was indicated by the load decrease at larger slips. The reason is that the M20 clamps are smaller and thus were prone to rotate as the beam moved. Some of the M20 clamps eventually disengaged from the steel beam as a result of substantial rotations.

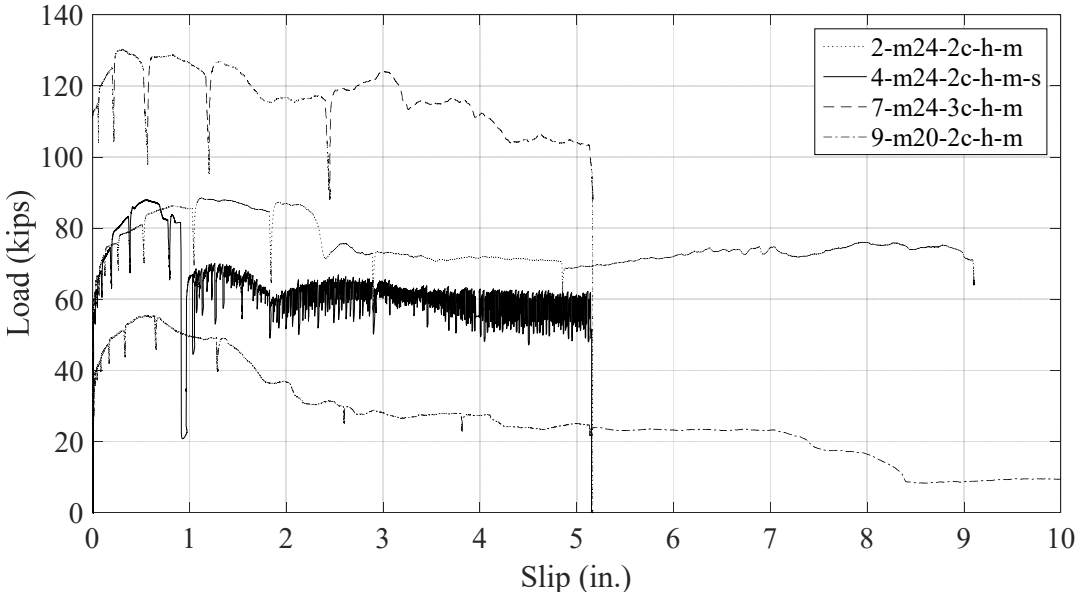

a) Monotonic Specimens

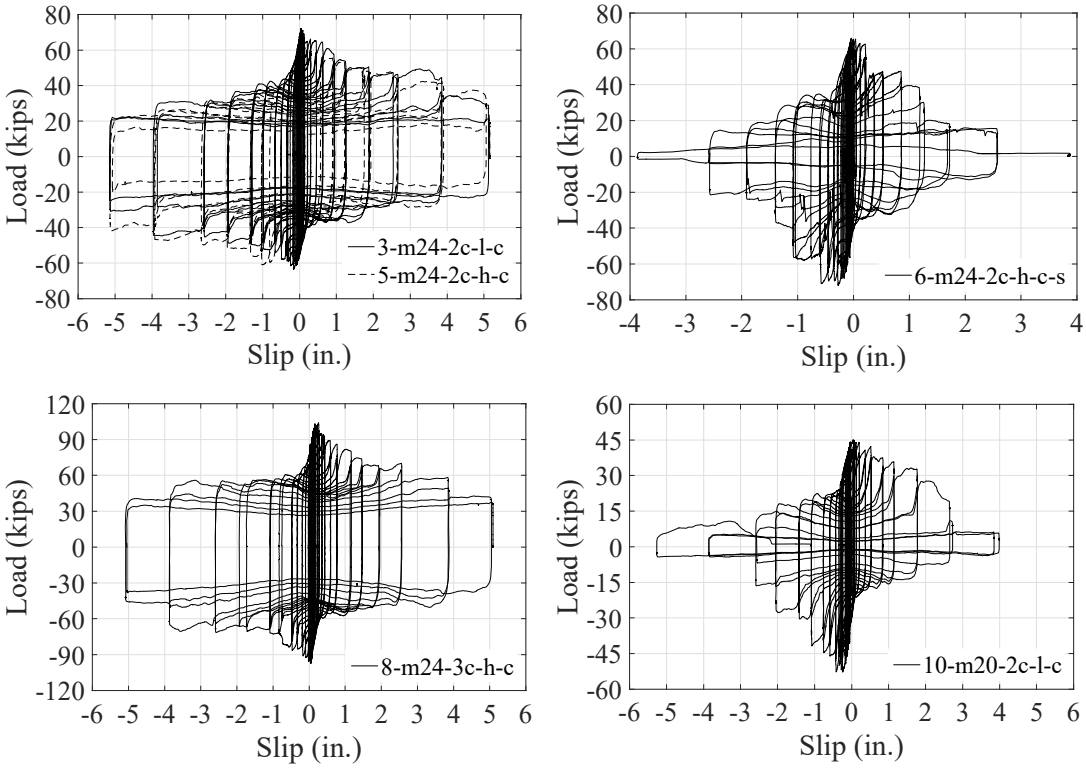

b) Cyclic Specimens

Figure 8. Load-Slip Curves

Table 4. Summary of Monotonic Test Results

Test	Slip load (kips)		Peak load (kips)		Load at 5 in. slip (kips)	
	Absolute	Normalized	Absolute	Normalized	Absolute	Percentage of peak load
2-m24-2c-h-m	60.8	1.00	88.5	1.00	68.9	78%
4-m24-2c-h-m-s	56.5	0.93	87.9	0.99	55.1	63%
7-m24-3c-h-m	87.0	1.43	130.1	1.47	104.0	80%
9-m20-2c-h-m	36.5	0.60	55.3	0.62	24.9	45%

The cyclic test results are summarized in Table 5. For the cyclic specimens, the peak loads at different slips are normalized relative to the peak strength of the corresponding monotonic specimens. Compared to the monotonic specimens, the peak strengths of the cyclic specimens were lower, but stabilized in a manner that may be addressed in design provisions. This is comparable to the decrease in strength seen in headed shear connectors when subjected to cyclic loading (Pallarés et al 2009). As the slip increased, the peak strength at each cycle decreased gradually, which could be attributed to the abrasion between the steel beam and the clamp and between the steel beam and the concrete plank. The abrasion may not only reduce the frictional coefficient but also release the bolt tension, because the damage to the clamp teeth and beam flange removes materials, reducing the clamping force and shear resistance at the contact surface. The results of Test 3-m24-2c-l-c and 5-m24-2c-h-c were plotted together to compare the behavior of specimens with different reinforcement configurations; the insignificant differences indicate that the light reinforcement was adequate and no anchor-related failure modes would occur. Because of the movement of the shims in Test 6-m24-2c-h-c-s and the large rotation of the M20 clamps in Test 10-m20-2c-h-c, their strengths decreased quickly at larger slips. As a result, less energy was dissipated in both tests. All the clamps ultimately detached from the steel beams in Tests 6-m24-2c-h-c-s and 10-m20-2c-h-c, while no specific limit states were observed for the remaining tests.

As exhibited in the load-slip curves, load oscillation caused by the stick-slip mechanism was observed in 4-m24-2c-h-c-s 4 and 6-m24-2c-h-c-s in which shims were used, although little loss in initial strength was seen. As such, usage of shims between the clamp and the flange may not be recommended in this application; further testing is recommended to confirm the behavior with shims between the clamps and the steel flange.

Table 5. Summary of Cyclic Test Results

Test	Slip (in.)	Peak load (kips)			
		Cycle 1		Cycle 2	
		Absolute	Normalized	Absolute	Normalized
3-m24-2c-l-c	0.16	69.4	0.78	66.9	0.76
	0.64	64.5	0.73	55.6	0.63
	2.56	47.5	0.54	46.1	0.52
	5.12	34.4	0.39	21.3	0.24
5-m24-2c-h-c	0.16	70.4	0.80	64.4	0.73
	0.64	57.2	0.65	48.6	0.55
	2.56	47.6	0.54	36.7	0.41
	5.12	37.4	0.42	23.1	0.26
6-m24-2c-h-c-s	0.16	65.5	0.75	59.2	0.67
	0.64	47.7	0.54	45.8	0.52
	2.56	15.9	0.18	15.7	0.18
	3.84	6.7	0.08		
8-m24-3c-h-c	0.16	104.0	0.80	97.4	0.75
	0.64	86.2	0.66	73.4	0.56
	2.56	70.2	0.54	63.6	0.49
	5.12	42.6	0.33	37.4	0.29
10-m20-2c-h-c	0.16	44.6	0.81	41.3	0.75
	0.64	42.3	0.76	37.4	0.68
	2.56	27.7	0.50	11.0	0.20
	3.84	6.3	0.11	6.1	0.11

Planned Beam Tests

- Test Setup

A full-scale composite beam test setup is illustrated in Figure 9. The test specimens consist of 30-foot W-shape beams, each with fifteen 2-ft.-wide planks attached using clamping connectors. The composite beam span is 30 ft., but the total beam length is 32 ft. due to 1 ft. extensions of the steel beam at each end to facilitate out-of-plane support and accommodate the deflection of the beam. The planks are 8 ft. long, which provides a sufficient composite slab width to prevent concrete premature failure in a narrow slab (Grant et al. 1977). The actuator force is spread using spreader beams to simulate uniform loading on the concrete slabs. Braces at both sides of the slab are engaged if the slab torques or displaces laterally due to uneven loading. Potential twisting of the steel beam is inhibited by the guides at the ends of the section. A pin support and a roller support are used to simulate the actual boundary conditions of a simple beam. Teflon sheeting is attached to surfaces where frictional forces are undesirable, such as the interface between the steel beam and the end guides.

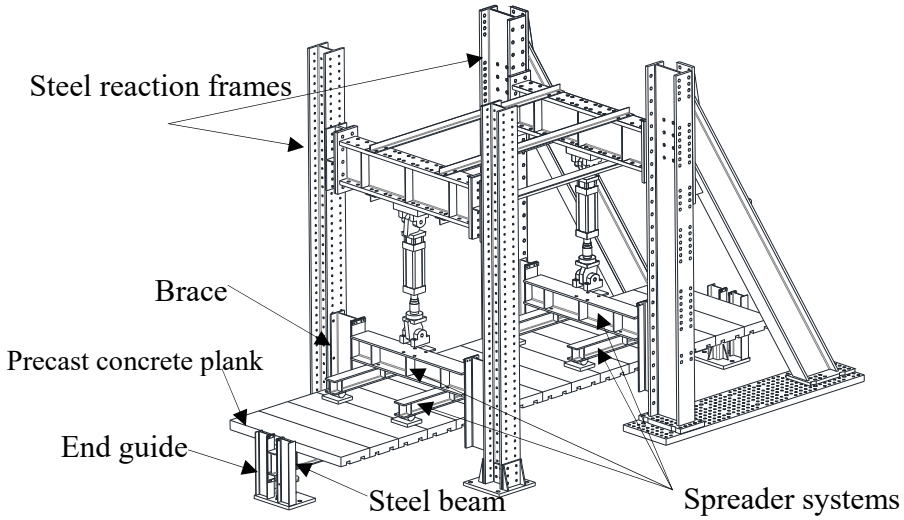

a) Three-dimensional view

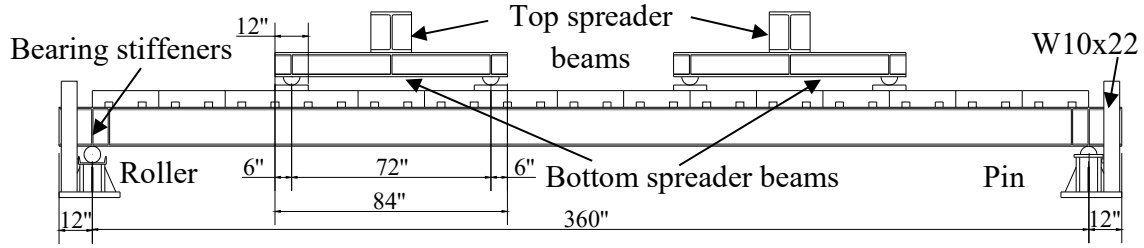

b) Elevation view

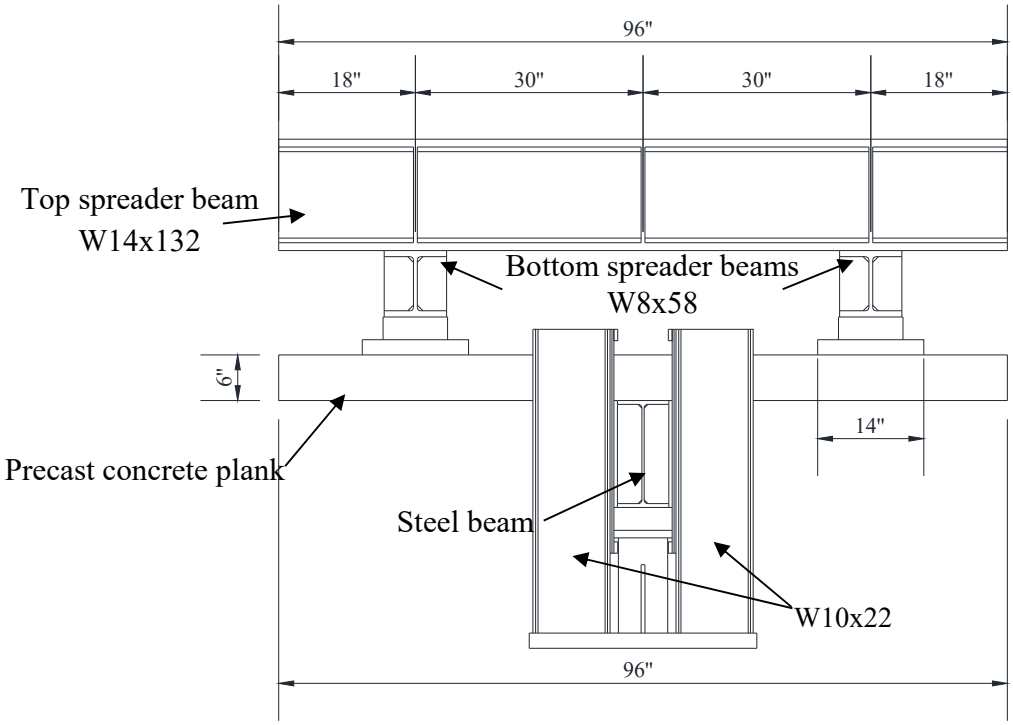

c) Side view

Figure 9. Different Views of Beam Test Specimen

A total of four specimens will be tested to document the progression of damage in the deconstructable composite beams (Table 6). The parameters include bolt diameter, number of channels per plank, steel beam section, and reinforcement configuration. The amount of composite action is also varied such that composite beams with a wide range of composite action can be investigated.

Table 6. Composite Beam Test Matrix

#	Bolt size (mm)	# of channels per plank	Steel beam section	Reinforcement configuration	Total number of bolts	Nominal percentage of composite action
1	24	2	W14x38	Heavy	60	118.5%
2	24	1	W14x38	Light	30	55.3%
3	20	3	W14x26	Light	90	158.2%
4	20	1	W14x26	Light	30	50.3%

CONCLUSIONS

A deconstructable composite floor system is proposed that enables sustainable design of composite beams and floors, deconstruction of buildings and reuse of the structural components. Composite action is achieved with clamped connections between precast planks and steel beams. Several T-bolts in the clamped connections were first tested to fracture to determine the number of turns of the nut for pretensioning. Two turns and 1.5 turns were found to be sufficient to ensure the yielding of the M24 and M20 bolts, respectively. Pushout tests were then conducted to document the load-slip curves of the clamped connections with various parameters. The load-slip curves indicate that the deconstructable clamping connectors using M24 bolts are ductile. Unlike the traditional shear studs that fracture at a much less slip, the M24 clamps retained almost 80% of the peak load at a slip of 5 in. in the monotonic test. Compared to the monotonic specimens, the strengths of the cyclic specimens were lower, but stabilized in a manner that may be addressed in design provisions. The strengths of the specimen with shims and the specimen with M20 clamps reduced quickly as slip increased, and thus less energy was dissipated. The behavior of specimens with different reinforcement configurations was similar, showing that the light reinforcement pattern, which excluded supplementary reinforcement placed around the channel anchors, was adequate. Shims were used for specimens with thin flange sections, and undesirable load oscillation was observed due to the stick-slip mechanism, although the strength was not affected. Full-scale beam tests are also designed which will explore the flexural behavior of the system under gravity loading.

ACKNOWLEDGMENTS

This material is based upon work supported by the National Science Foundation under Grant No. CMMI-1200820, the American Institute of Steel Construction, Northeastern University, and Simpson Gumpertz & Heger. In-kind support is provided by Benevento Companies, Capone Iron Corporation, Fastenal,

Halfen, Lehigh Cement Company, Lindapter, Meadow Burke, and S&F Concrete. This support is gratefully acknowledged. The authors would like to thank Kyle Coleman, Michael McNeil, Kurt Braun, Corinne Bowers, Edward Myers, Majed Alnaji, Michael Bangert-Drowns, Kara Peterman, Angelina Jay, Justin Kordas, David Padilla-Llano, and Yujie Yan for their assistance with the experiments. Any opinions, findings, and conclusions expressed in this material are those of the authors and do not necessarily reflect the views of the National Science Foundation or other sponsors.

REFERENCES

AISC (2010a). *Specification for Structural Steel Buildings*, American Institute of Steel Construction, Chicago, Illinois.

Grant, J. A., Fisher, J. W., and Slutter, R. G. (1977). "Composite beams with formed steel deck," *Engineering Journal*, Vol. 14, No.1, pp. 24-43.

Pallarés, L. and Hajjar, J. F. (2009). "Headed Steel Stud Anchors in Composite Structures: Part I. Shear," Report No. NSEL-013, Newmark Structural Laboratory Report Series (ISSN 1940-9826), Department of Civil and Environmental Engineering, University of Illinois at Urbana-Champaign, Urbana, Illinois, April.

RCSC (2009). *Specification for Structural Joints Using High-Strength Bolts*, Research Council on Structural Connections, Chicago, Illinois.

Wang, L., Webster, M. D., and Hajjar, J. F. (2015). "Behavior of Deconstructable Steel-Concrete Shear Connections in Composite Beams," Proceedings of the 2015 SEI Structures Congress, Portland, Oregon, April 23-25, 2015, ASCE, Reston, Virginia.

Webster, M., Kestner, D., Parker, J., Johnson, M. (2007) "Deconstructable and Reusable Composite Slab," Winners in the Building Category: Component – Professional Unbuilt, Lifecycle Building Challenge <http://www.lifecyclebuilding.org/2007.php>